A RADIO-CONTROLLED ORNICOPTER MODEL

Monique Heiligers, Stijn van den Bulcke, Theo van Holten, Rolf Kuiper
Delft University of Technology
Kluyverweg 1, 2629 HS Delft, The Netherlands

Abstract

The Ornicopter is a single rotor helicopter without a reaction torque. By forcing the blades of the Ornicopter to flap up and down, both a lifting force and an average propulsive force can be generated. Because of this average propulsive force the blades will propel (i.e. rotate) themselves and there will no longer be a need to transfer torque from the fuselage to the rotor. If there is no longer a torque transferred from the fuselage to the rotor there will neither be a reaction torque.

This paper will present the design and testing of a radio-controlled Ornicopter model. Design criteria regarding vibrations, spring stiffness of the system and flexibility of the blades will be identified. Subsequently the design of the forced flapping mechanism and yaw control system will be explained. The tests will demonstrate the torqueless operation of the Ornicopter and will give insight into the lift that is produced and the amount of yaw control that is achievable.

c	Blade chord
c_{l_α}	Derivative of c_l with respect to α $dc_l/d\alpha$
k	$k^2=EI/m\Omega^2R^4$
m	Mass per unit length
m_{fl}	Non-dimensional flapping moment
$\hat{m}_{fl}$	Amplitude of the non-dimensional flapping moment
r	Radius of blade element
v_i	Induced velocity
x	Non-dimensional radius of blade element r/R
C_l	Lift coefficient of a blade
E	Modulus of elasticity
I	Mass moment of inertia of the rotor blade about the rotor hub
L	Lift
M_a	Aerodynamic moment
M_{fl}	Mechanical flapping moment
P_a	Power available to drive the rotor
P_{eng}	Engine power, power transmitted by the engine to the spring of the mechanical flapping mechansim
P_{fl}	Mechanical flapping power, power exerted by the flap forcing mechanism on the blade
P_p	Power required to overcome the profile drag
Q	Torque about the rotor hub
R	Rotor radius
Z	Vertical displacement of the flexible rotor blade
α	Angle of attack
α	Southwell coefficient
β	Flapping angle of the blade
$\hat{\beta}$	Amplitude of the flapping angle
β'	Derivative of β with respect to the azimuth angle $d\beta/d\psi$
β''	Second derivative of β with respect to the azimuth angle $d^2\beta/d\psi^2$
$\dot{\beta}$	Derivative of β with respect to time $d\beta/dt$
$\ddot{\beta}$	Second derivative of β with respect to time $d^2\beta/dt^2$
ε	Angle between the horizontal and the line tangent to the blade curvature at the blade root, or $\varepsilon = dZ(r=0)/dr$
$\dot{\varepsilon}$	Derivative of ε with respect to time $d\varepsilon/dt$
$\hat{\varepsilon}$	Amplitude of the angle between the horizontal and the line tangent to the blade curvature at the blade root
γ	Lock number $\rho C_{l_\alpha} cR^4/I$
φ	Inflow angle
λ_i	Non-dimensional induced velocity $v_i/\Omega R$
θ	Pitch angle
ρ	Air density
ψ	Azimuth angle
ω_n	Natural frequency
ω_{nr}	Non-rotating natural frequency
Ω	Rotational speed of the rotor

Introduction

The tail rotor of helicopters, necessary to counteract the reaction torque of the engine and to control the helicopter in yaw, has always been considered a necessary evil. It is expensive, consumes power, has only marginal control authority under unfavorable wind conditions, and is on top of that noisy, vulnerable and dangerous. The ideal solution to all these problems would be to design a rotor that eliminates the need for a tail rotor. The Ornicopter is such a revolutionary design.

The mechanism of the Ornicopter is derived from bird flight. When birds flap their wings they are able to derive both a lifting force and a propelling force out of it. Instead of propelling a helicopter blade by spinning it around and deriving lift from this rotating movement, as is done in conventional helicopter configurations, the Ornicopter flaps its

blades like a bird and derives both lift and a propulsive force from this movement. In this case the blades propel (i.e. rotate) themselves and there is no longer a need for a direct torque supplied by the engine to rotate the blades. The fact that the engine torque is no longer directly transferred from the fuselage to the rotor is the key feature of the Ornicopter, and it is this feature that makes the anti torque device redundant.

How lift is derived from forced flapping

As stated before, the Ornicopter should flap its blades like bird wings in order to obtain both a propulsive force that will rotate the blades and a lift force that will keep the Ornicopter airborne. The movement of a bird wing however is extremely complicated and it is impossible to mimick this movement exactly with an Ornicopter blade. But a very useful and simple approximation can be obtained by applying a constant pitch angle to the Ornicopter blade.

The movement of an Ornicopter blade during one revolution is pictured in figure 1. During one revolution of the blade, the blade will be forced to flap both up and down once, resulting in the shown undulating path. If a constant pitch angle is applied the lift forces during one revolution will (averaged over one revolution) result in an upward force and an average propulsive force. This average propulsive force is achieved because the forward horizontal component of the lift force that occurs when the blade is flapping downwards is much larger than the backward horizontal component of the lift force that occurs when the blade is flapping upwards. Thus by setting all the Ornicopter blades at a constant pitch angle and flapping them upwards and downwards a propulsive force is created that will rotate the blades around the rotor hub and an upward force is created that will counteract gravity.
For a further explanation of the basic principles of the Ornicopter (a calculation of the power required, or an explanation of yaw control, cyclic control and collective control) see (Ref 1 and 2).

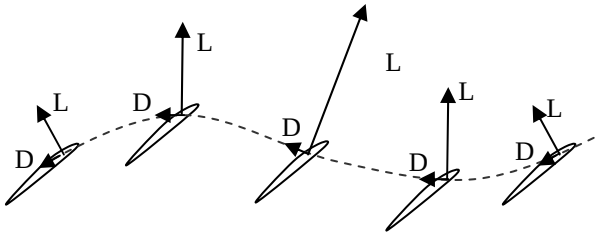

Figure 1: Lift and drag forces acting on an Ornicopter blade during one revolution when a constant pitch angle is applied.

Ornicopter design formulas

This section will introduce the Ornicopter design formulas regarding the amount of flapping power that needs to be transmitted to the blade, the magnitude of the required forced flapping angles and the magnitude of the forced flapping moment. These design formulas will be used later on in this paper to calculate the magnitude of these quantities for the demonstrator model.

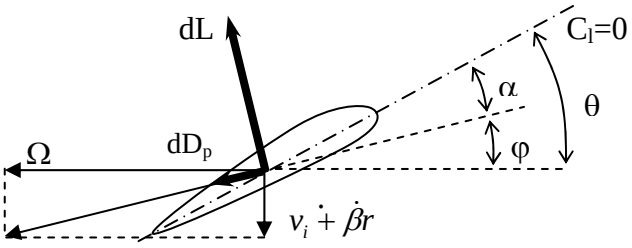

Figure 2: Aerodynamic forces and velocities on a blade element at distance *r* from the rotor hub

Required flapping power

To calculate the power that is needed to drive the Ornicopter rotor, the power needed to drive the blade element in figure 2 is calculated, and integrated over the entire rotor blade. To find the average power during one revolution, the power is integrated over one revolution and divided by the factor 2π. This yields, assuming small angles:

$$P_{sh} = \frac{1}{2\pi}\int_0^{2\pi} d\psi \int_0^R \left(dL\varphi + dD_p\right)\Omega r \qquad (1)$$

with the inflow angle φ given by:

$$\varphi = \frac{v_i + \dot{\beta} r}{\Omega r} \qquad (2)$$

Substitution of equation (2) into equation (1) gives:

$$P_{sh} = \frac{1}{2\pi}\int_0^{2\pi} d\psi \int_0^R dL\left(v_i + \dot{\beta} r\right) + \frac{1}{2\pi}\int_0^{2\pi} d\psi \int_0^R dD_p \Omega r \qquad (3)$$

$$P_{sh} = P_i + P_p + \frac{1}{2\pi}\int_0^{2\pi} M_a \dot{\beta} d\psi \qquad (4)$$

in which P_i is the power required to overcome the induced drag, P_p the power required to overcome the profile drag, and M_a the aerodynamic flapping moment:

$$P_i = \frac{1}{2\pi}\int_0^{2\pi} d\psi \int_0^R dL v_i \qquad (5)$$

$$P_p = \frac{1}{2\pi}\int_0^{2\pi} d\psi \int_0^R dD_p \Omega r \qquad (6)$$

$$M_a(\psi) = \int_0^R dL r \qquad (7)$$

Equation (4) is a power equation that can be used for conventional helicopters, but note that $\dot{\beta}$ will be zero for a conventional helicopter during hover. To be able to add the mechanical flapping power to equation (4), consider the equation of motion for a centrally hinged rotor blade in Ornicopter configuration, i.e. with a mechanical flapping moment (M_{fl}) applied to the blade. The equation of motion can be expressed as (see figure 3):

$$\ddot{\beta} + \Omega^2 \beta = \frac{M_a}{I} + \frac{M_{fl}}{I} \tag{8}$$

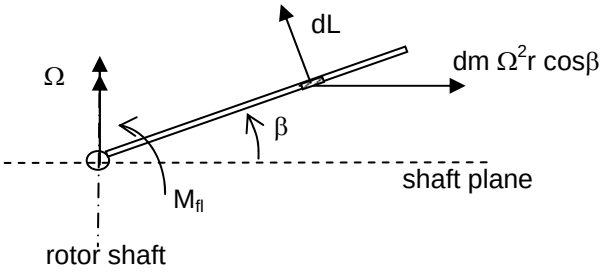

Figure 3: Moments and forces on an Ornicopter blade with mechanical flapping moment applied to the blade

If the forced flapping frequency is chosen equal to the 1-P frequency of the blade, then the flapping angle will in response also have a 1-P frequency and will be given by:

$$\beta = \beta_0 + C\cos\psi + S\sin\psi \tag{9}$$

β_0 is the cone angle. Equation (8) now yields:

$$M_a = -M_{fl} + I\Omega^2\beta_0 \tag{10}$$

When combining equations (10) and (4):

$$P_{sh} = P_i + P_p - \frac{1}{2\pi}\int_0^{2\pi}\left(M_{fl} - I\Omega^2\beta_0\right)\dot{\beta}d\psi \tag{11}$$

$$P_{sh} = P_i + P_p - P_{fl} \tag{12}$$

$$P_{fl} = \frac{1}{2\pi}\int_0^{2\pi}\left(M_{fl} - I\Omega^2\beta_0\right)\dot{\beta}d\psi \tag{13}$$

In which P_{fl} denotes the flapping power: the average power per revolution exerted by the flap forcing mechanism on the blade. Equation (12) shows that if the flapping power (P_{fl}) is chosen sufficiently large, the shaft power can be reduced to zero. This means that if the rotor is driven by the flap forcing mechanism, there will be no need for any additional shaft power (engine power however will still be needed for the flapping of the blades). So, for the Ornicopter situation, equation (11) transforms into:

$$0 = P_i + P_p - \frac{1}{2\pi}\int_0^{2\pi}\left(M_{fl} - I\Omega^2\beta_0\right)\dot{\beta}d\psi \tag{14}$$

$$0 = P_i + P_p - P_{fl} \tag{15}$$

It can thus be seen that the flapping power has to replace the shaft power, and that the flapping power will thus not be larger than the power that is transferred to the rotor in conventional helicopters.

Required mechanical flapping moment and flapping angle

The power equations (12) and (13) together with the equation of motion (8) and the expression for the aerodynamic moment (equation (10)) can be used to find an expression for the mechanical flapping moment M_{fl} and the flapping angle β during hover. In order to do so, the aerodynamic moment is expressed as (see also figure 2):

$$M_a = \int_0^R c_{l_\alpha}\alpha\frac{1}{2}\rho(\Omega r)^2 c r dr \tag{16}$$

$$M_a = \int_0^R c_{l_\alpha}\left[\theta - \frac{v_i}{\Omega r} - \beta'\right]\frac{1}{2}\rho(\Omega r)^2 c r dr \tag{17}$$

$$M_a = \frac{1}{2}\frac{\rho C_{l_\alpha} c R^4}{I} I\Omega^2 \int_0^1 \left(\theta - \frac{\lambda_i}{x} - \beta'\right)x^3 dx \tag{18}$$

$$M_a = \frac{\gamma}{2} I\Omega^2\left(\frac{\theta}{4} - \frac{\lambda_i}{3} - \frac{\beta'}{4}\right) \tag{19}$$

with x the non-dimensional rotor radius, γ the Lock number, β' the derivative of the flap angle w.r.t. the azimuth angle and λ_i the non-dimensional induced velocity defined as:

$$x = \frac{r}{R} \tag{20}$$

$$\gamma = \frac{\rho C_{l_\alpha} c R^4}{I} \tag{21}$$

$$\beta' = \frac{d\beta}{d\psi} = \frac{d\beta}{d\Omega t} = \frac{\dot{\beta}}{\Omega} \tag{22}$$

$$\lambda_i = \frac{v_i}{\Omega r} \tag{23}$$

If the non-dimensional aerodynamic flapping moment (m_a) and the non-dimensional mechanical flapping moment (m_{fl}) are defined by:

$$m_a = \frac{M_a}{\Omega^2 I} \tag{24}$$

$$m_{fl} = \frac{M_{fl}}{\Omega^2 I} \tag{25}$$

then, using equations (19), (24) and (25) equation (10) can be written as:

$$m_{fl} = -\frac{\gamma}{2}\left(\frac{\theta}{4} - \frac{\lambda_i}{3} - \frac{\beta'}{4}\right) + \beta_0 \tag{26}$$

Now assume that:

$$m_{fl} = A\cos\psi + B\sin\psi \tag{27}$$

Substitution of equations (9) and (27) into (26) gives:

$$A\cos\psi + B\sin\psi = -\frac{\gamma}{8}\theta + \frac{\gamma}{6}\lambda_i + \frac{\gamma}{8}\left(-C\sin\psi + S\cos\psi\right) + \beta_0 \quad (28)$$

It can now be seen that:

$$A = \frac{\gamma}{8}S \quad (29)$$

$$B = -\frac{\gamma}{8}C \quad (30)$$

Thus, the non-dimensional mechanical flapping moment as a function of the flapping coefficients is given by:

$$m_{fl} = \frac{\gamma}{8}S\cos\psi - \frac{\gamma}{8}C\sin\psi \quad (31)$$

By combining equations (9), (27), (29) and (30) a relation can be found between the amplitude of the flapping angle ($\hat{\beta}$) and the amplitude of the non-dimensional flapping moment ($\hat{m}_{fl}$):

$$\hat{m}_{fl} = \sqrt{A^2 + B^2} = \frac{\gamma}{8}\hat{\beta} \quad (32)$$

The final step is to substitute equations (9), (27) and (32) into the expression for the flapping power (13):

$$P_{fl} = \frac{I\Omega^3}{2}\frac{\gamma}{8}\hat{\beta}^2 = \frac{I\Omega^3}{2}\frac{8}{\gamma}\hat{m}_{fl}^2 \quad (33)$$

Recapitulating, since P_i and P_p can be calculated, equation (15) gives an expression for the flapping power P_{fl}. Once P_{fl} is known, equation (33) can be used to calculate the required amplitude of the mechanical flapping angle and non-dimensional flapping moment.

Windtunnel tests

Windtunnel tests have been performed as a first check on the developed theory (see also Ref 1, 2, 3 and 4) and the feasibility of the Ornicopter. The results of these windtunnel tests which are important for the design of the demonstrator model will be briefly summarized in this section, for an elaborate discussion see (Ref 2).

As one of the most important results the windtunnel model (see figure 4)proved that reaction-less operation of the Ornicopter indeed is possible. A torqueless situation was achieved while the rotor was still producing a lifting force, see figure 5. Moreover, the torqueless situation was obtained while using only modest flapping angles, in the order of 12 degrees.

Figure 5 also shows that yaw control is still possible: both a negative and a positive reaction torque can be achieved which will result in a yaw movement in one way or the other.

However, the windtunnel model also demonstrated three points of attention that required further research and needed to be improved.

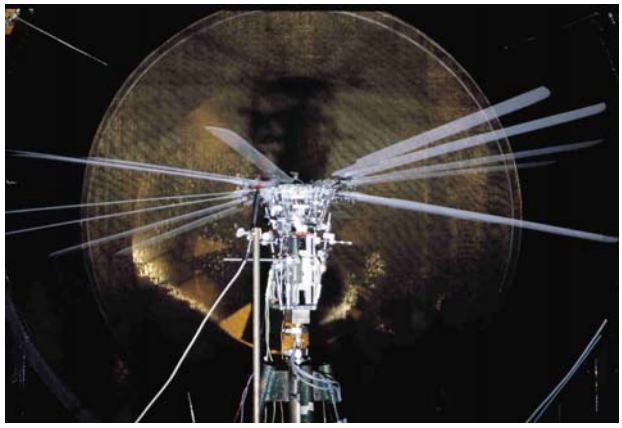

Figure 4: Ornicopter windtunnel model

First, the windtunnel tests indicated that a considerable amount of power was lost due to the friction in the forced flapping mechanism: 5 Watts was lost due to friction on a total of 10 Watts. It should be noted here that the wintunnel model was not optimized for friction, and therefore these results could have been expected. However, this clearly indicated that it is of utmost importance to keep the friction, and thus the power loss, within the forced flapping mechanism as low as possible. Otherwise the flapping mechanism itself might require more power than the amount of power that can be saved due to the fact that a tail rotor (or other anti torque device) is no longer necessary.

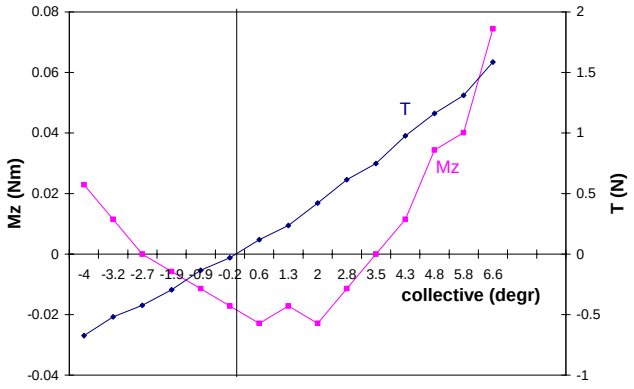

Figure 5: Rotor torque (M_z) and rotor thrust (T) as a function of collective pitch for a double teeter Ornicopter with twelve degrees flapping

The second point of attention concerned the flapping configuration that was used for the windtunnel tests. The rotor of the windtunnel model was based on the double teeter flapping configuration as shown in figure 6. As indicated by

its name, the rotor consists of two teeters: the two opposite blades are connected like a see-saw, which means that if one blade is flapping upwards, the opposite blade is flapping downwards. All four of the blades are forced to flap with a 1-P frequency. At the moment in time that one of the two teeters is at its maximum flapping angle, the other teeter will be in the neutral position, as shown in figure 6. The tip path planes of the two teeters are anti-symmetrically tilted with respect to the shaft.

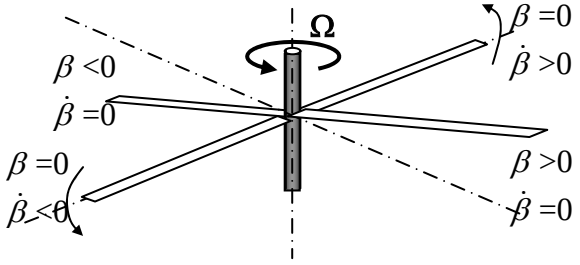

Figure 6: Principle of the four bladed double teeter rotor.

During the windtunnel tests it became clear that the double teeter configuration appeared to cause some severe vibrations. Calculations (Ref 3) showed that a double teeter configuration causes a 2-P vibration in the roll and pitch moment, and a 2-P vibration on the in-plane forces. In order to eliminate these vibrations another flapping sequence of the rotor blades is desirable.
And finally the flapping angles that were necessary for torqueless operation of the Ornicopter windtunnel model were larger than expected from theory (Ref 4). Using the formula for the required flapping power (equation 33) a required flapping angle was calculated in the order of 8 degrees. For the windtunnel model a flapping angle of 12 degrees appeared to be necessary, although the amount of flapping *power* that was applied to the Ornicopter blades was still consistent with the calculated theoretical value. This difference could be explained by the flexibility of the blades. The theoretical calculations were based on the assumption of rigid rotor blades, whereas in reality the rotor blades have some degree of flexibility. Flexible blades do not require additional power, but do require a larger forced flapping angle at the root of the blade (the deflection of the tip of the flexible blade however is equal to the deflection of the tip of a rigid blade). The next section will elaborate some more on the influence of the flexibility of the blades.

Design criteria for the demonstrator model

Using the results from the developed theory and the results from the windtunnel tests some important design criteria can be set. Design criteria regarding minimizing vibrations, regarding the influence of flexibility of the blades and regarding requirements for the spring stiffness of the entire system.

Vibrations

In order to eliminate (or at least reduce) the vibrations that are caused by a double teeter configuration, another rotor configuration (i.e. flapping sequence of the blades) was looked for. The rotor configuration that caused the least vibrations appeared to be the so called 2x2 anti-symmetrical configuration (Ref 3).

The rotor in anti-symmetrical configuration also consists of four blades, but now the two opposite blades are flapping in the same direction. So (looking at figure 7) if blade *k=0* is flapping upwards, blade *k=2* is flapping upwards as well, while at the same time the two other blades will be flapping downwards, and vice versa. The blades will pass through the neutral position at the same moment in time.

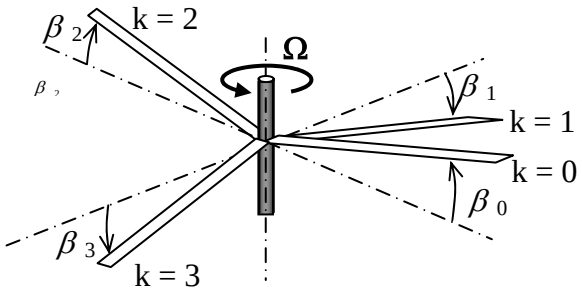

Figure 7: Principle of the 2x2 anti-symmetrical rotor

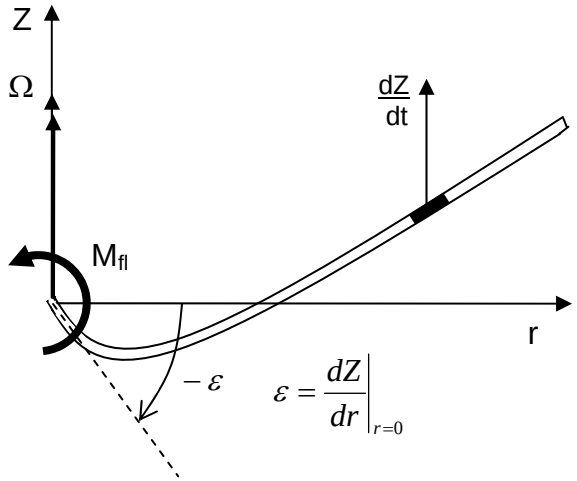

Figure 8: Schematic representation of a flexible blade with forced flapping mechanism

The only vibration that will occur within a 2x2 anti-symmetrical configuration is a 2-P vibration on the torque (Ref 3). This vibration is caused both by inertia forces (change of angular momentum) and by aerodynamic forces. Vibrations in roll moment, pitch moment, in-plane forces and vertical force do not occur. It should also be noted that the 2-P

vibration on the torque that does occur is not an unusual vibration: it is also present in single teeter rotors.

The free-flying demonstrator model will thus be constructed as a 2x2 anti-symmetrical rotor.

Flexibility of the blades

As stated before, the windtunnel tests indicated that, when flexible blades are incorporated instead of the theoretical rigid blades, the flapping mechanism should allow for a larger forced flapping angle at the root of the blades than predicted by theory. This effect has been studied more extensively in order to be able to predict the difference in the magnitude of the flapping angle more accurately (Ref 4). The most important findings of this study for design purposes will be briefly explained below.

Within this study the flexible blade is modeled using a two-mode approximation, and it is assumed that the blade is centrally hinged and is forced to flap by a flapping moment that acts at the very root of the blade (see figure 8). The resulting flapping motion of the flexible blade during one revolution around the rotor hub is depicted in figure 9. As a reference the flapping motion of a rigid blade (that was used to calculate the theoretical value) that is excited by the same flapping moment is also plotted in figure 9.

As a first comment it is noted that no power is lost due to the flexibility of the blades. All flapping power that is transferred to the root of the blade is converted into power available (the forward component of the lift that is propelling the rotor blade multiplied by the angular velocity).

Further figure 9 immediately shows that the angle at the root of the flexible blade is indeed larger than the blade root angle of the rigid blade, while the tip deflection is almost equal for both blades. To obtain these results a non-dimensional stiffness for the flexible blade was assumed in the calculations equal to:

$$k^2 = \frac{EI}{m\Omega^2 R^4} = \frac{1}{270} \qquad (34)$$

and, as a result, the ratio between the flexible blade root angle and rigid blade root angle appeared to be equal to:

$$\frac{\hat{\varepsilon}_{flex}}{\hat{\varepsilon}_{rigid}} = \frac{\hat{\varepsilon}_{flex}}{\hat{\beta}} = 5 \qquad (35)$$

This ratio is much larger than the ratio found during the windtunnel tests (which was equal to 1.5). It should therefore be mentioned that the situation considered in the theoretical study (as depicted in figure 8) actually is a worst case scenario. The ratio will drop if the blade is not centrally hinged but at an offset (as was the case in the windtunnel model). The ratio will also drop when the forced flapping moment is not applied at the exact location of the root, but at a certain distance away from the root (to the right of the root in figure 5), this was also the case for the windtunnel model. And naturally, when the blades have a larger stiffness than assumed in equation (34) this will also decrease the ratio. The blades of the windtunnel model indeed had a larger stiffness. As a final factor contributing to a lower ratio it can be mentioned that in order to transfer the same amount of flapping power to the flexible blade a smaller mechanical flapping moment will be required than for the rigid blade since the blade root angle is larger which results in a larger angular velocity ($\dot{\varepsilon}$), see also figure 8:

$$P_{fl} = \frac{1}{2\pi}\int_0^{2\pi} M_{fl}\,\dot{\varepsilon}\,d\psi \qquad (36)$$

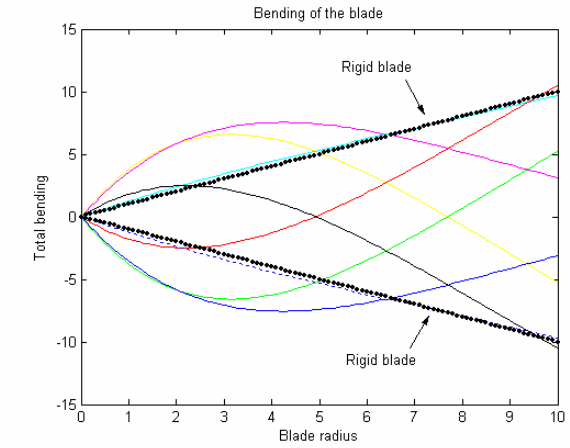

Figure 9: Bending of a flexible blade (an azimuth angle difference of $\pi/4$ occurs between two successive plots) and a rigid blade for a given flapping moment

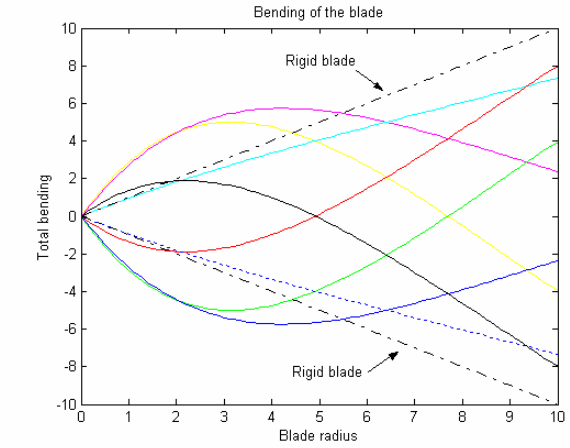

Figure 10: Bending of a flexible blade and a rigid blade for the same flapping power

Thus, instead of comparing the motion of a rigid and flexible blade for the same flapping *moment* (as is done in figure 9), it is more correct to compare the motion of a rigid and flexible blade

that consume the same amount of flapping *power* and produce the same amount of propelling force and lifting force, this is done in figure 10. Figure 10 illustrates that this effect will also decrease the ratio between blade root angle of a flexible and rigid blade.

For practical applications it can thus be concluded that, as long as the blade root angle that is calculated from equation (33) necessary to produce a certain amount of flapping power and power available is multiplied by a factor 5, and the forced flapping mechanism can allow for this larger blade root angle the design will suffice, and will be on the safe side.

The spring stiffness of the system

Irrespective of the fact whether springs are incorporated in the forced flapping mechanism, or whether the flexibility of the blades is sufficient to allow for the superposition of the conventional flapping motion on the forced flapping motion, there are some requirements for the spring stiffness of the entire system (blade and flapping mechanism together).

The maximum response of the rotor should follow its maximum force input by a phase angle of approximately 90 degrees. If the phase angle deviates too much from 90 degrees too much (unwanted) flapping cross-coupling will occur, this basically means that when a control input is given in the longitudinal direction it will have a side effect in the lateral direction which needs to be cancelled by the pilot by giving an additional lateral control input.

The phase angle (φ) depends on the frequency ratio (ν) and the Lock number as shown in figure 11. The frequency ratio is the ratio between the rotational frequency (Ω) and natural frequency (ω_n) of the blade. The natural frequency (ω_n) of a hinged rotor blade without offset is identical to its rotational frequency (Ω) and therefore the phase angle will always be exactly 90 degrees (see figure 11). If springs are incorporated in the mechanism or if an offset is applied, then the natural frequency of the blade will no longer be equal to the rotational frequency and as a result the phase angle will start to deviate. Due to the offset or springs, the natural frequency will increase and as a consequence the frequency ratio will become smaller than 1.

Since the phase angle should not deviate too much from 90 degrees a requirement can be set that the frequency ratio should not become smaller than 0.9:

$$\nu = \frac{\Omega}{\omega_n} > 0.9 \tag{37}$$

or

$$\omega_n < 1.1\Omega \tag{38}$$

According to Southwell the natural frequency of a blade can be expressed as follows:

$$\omega_n^2 = \omega_{nr}^2 + \alpha\Omega^2 \tag{39}$$

In this equation ω_{nr} is the non-rotating natural frequency and α the Southwell coefficient which incorporates the effects of springs and/or hinge offset.

The hinge offset and spring stiffness of the springs in the flapping mechanism and/or the flexibility of the rotor blades should thus be chosen such that equation (38) is true.

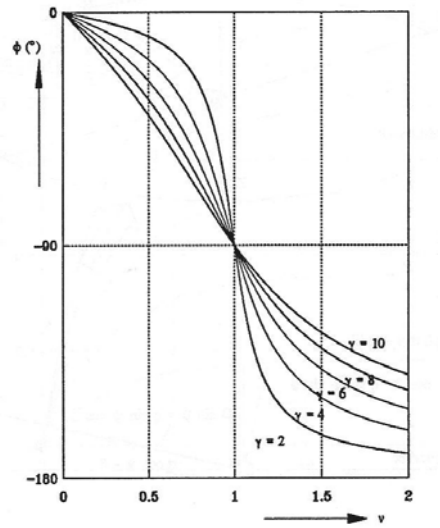

Figure 11: Phase angle as a function of the frequency ratio and Lock number

Design of the demonstrator model

This section will focus on the actual design of the demonstrator model. It will begin with an explanation of the helicopter kit that has been chosen as a starting point, followed by a description of the forced flapping mechanism that will have to ensure the desired flapping sequence of the blades. Subsequently the corresponding values for the flapping power, flapping angle and flapping moment the design will have to cope with will be calculated. After that the spring stiffness of the flapping mechanism will be checked, and finally the resulting final design will be presented.

Chosen configuration

As explained in the previous section the 2x2 anti-symmetrical configuration was chosen for the demonstrator model due to its favorable vibration characteristics. The rotor of the demonstrator model will thus consist of four blades.

Chosen helicopter kit

The helicopter kit that was chosen as a starting point to build a scale-model Ornicopter is the Vario X-treme economic (Max RPM 1500, Rotor diameter 1.5 m, number of blades: 2). This kit will be fitted with a slightly larger engine than recommended by the manufacturer: 11.5cc instead of 10cc. The two rotor blades will be replaced by the blades of a four bladed Vario rotor in order to be able to achieve a 2x2 anti-symmetrical configuration.

Design of the forced flapping mechanism

The basic principles of the forced flapping mechanism that has been developed for the demonstrator model will be explained below.

The gearwheel mechanism. A forced flapping mechanism will have to be added to the helicopter kit that will force the four blades to flap up and down in the exact sequence of the 2x2 anti-symmetrical configuration. For this purpose a flapping mechanism was designed based on five gearwheels that are placed in a planetary system, see figure 12.

The center gearwheel is fixed and does not rotate, the other four gearwheels are forced to rotate around the center gearwheel with the angular velocity of the rotor (Ω). This implies that each of the outer gearwheels itself has an angular velocity equal to 2Ω with respect to a fixed reference frame.

Figure 13 indicates what exactly happens to one of the outer gearwheels during one complete rotation

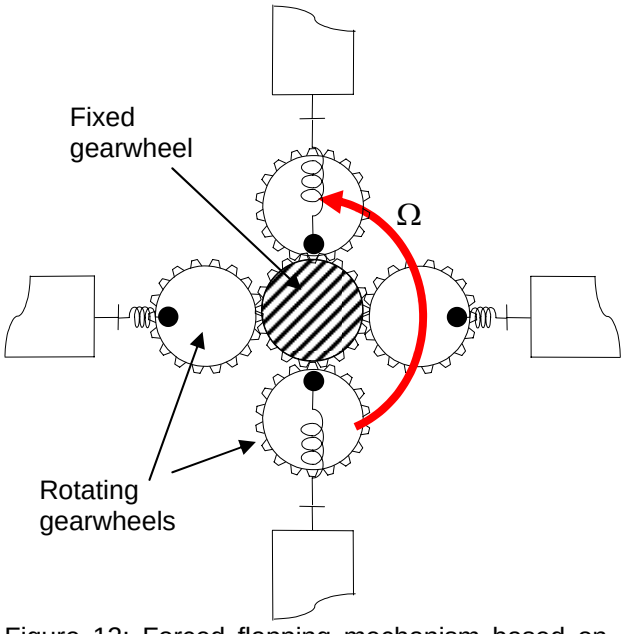

Figure 12: Forced flapping mechanism based on planetary gearwheels

around the fixed center gearwheel: when the outer gearwheel has made half a revolution around the center gearwheel, then the outer gearwheel itself has made a complete revolution with respect to a fixed reference frame.

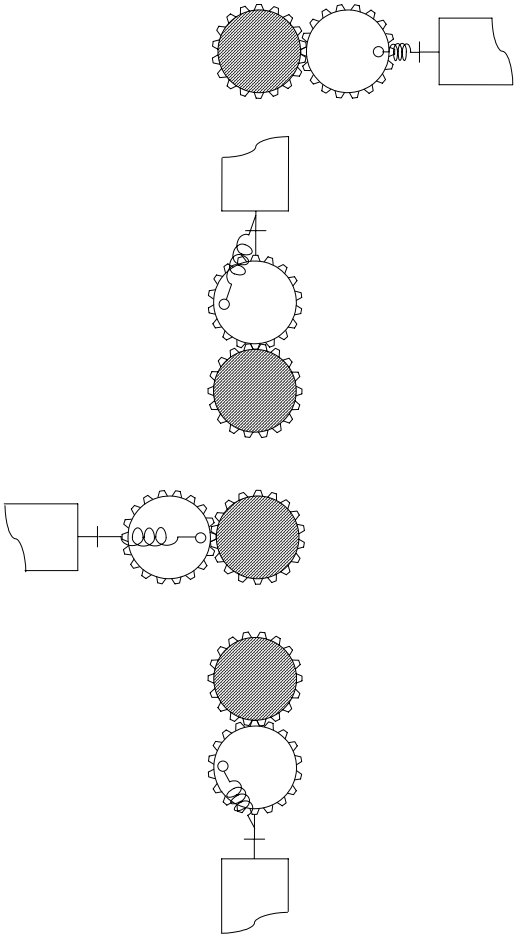

Figure 13: Outer gearwheel during one revolution around the center gearwheel

To introduce a forced flapping motion into the blade one side of a spring is attached to the blade and the other end of the spring is attached to a small pin that is located on the surface of the outer gearwheel. It can be seen that during one complete revolution of the blade around the fixed center gearwheel the spring is compressed, goes back to neutral, is stretched and goes back to neutral again (figure 13). This means that the blade is first forced to flap down, goes back to neutral, is forced to flap up and goes back to neutral again. A 1-P forced flapping motion is thus achieved.

By carefully choosing the starting position of all gearwheels, or actually the starting position of the attachment points on all the gearwheels, the situation can be created that two opposite blades are flapping upwards while at exactly the same moment in time the two other blades are flapping downwards. Such a starting position is shown in

figure 12. When the gearwheels start rotating from this initial condition a 2x2 anti-symmetrical configuration is achieved.

The forced flapping mechanism. To increase clarity in the drawings, the principle of the forced flapping mechanism has been explained using springs. For the demonstrator model push pull rods will be used instead of springs. This however will not change the working of the mechanism.

The flapping mechanism as designed for the demonstrator model is shown in figure 14. For clarity only one planet gearwheel and one blade-holder are shown, in reality the flapping mechanism will of course consist of four planet gearwheels, four blade-holders and four blades. It should also be noticed that in figure 14 not only the planet gearwheel is rotating around the fixed gearwheel, but the entire structure. The upper plate, lower plate, blade-holder, blade, lever and planet gearwheel are all rotating around the fixed axis and fixed gearwheel.

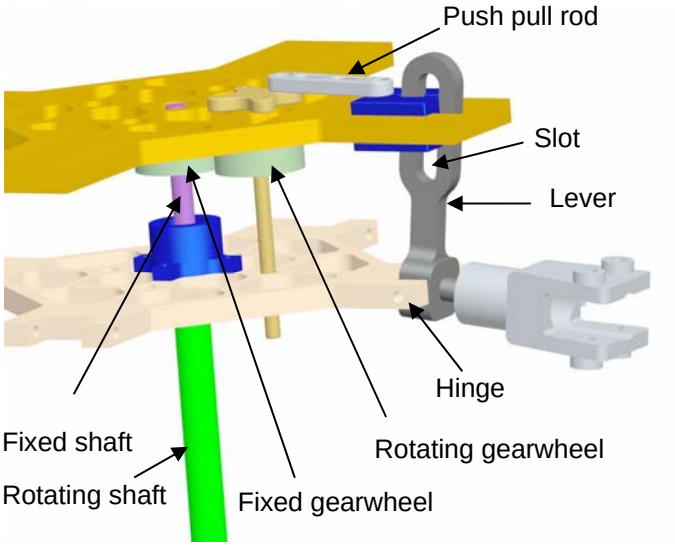

Figure 14: The forced flapping mechanism used in the radio-controlled demonstrator model

Yaw control. Yaw control is achieved by so called 'over-flapping' or 'under-flapping' of the rotor blades thereby deliberately introducing a small amount of reaction torque. Within the flap forcing mechanism of the demonstrator model the forced flapping angle can be changed by shifting the position of the upper plate in figure 14 upwards or downwards.
Since the push pull rod has a fixed stroke a shift of the upper plate upwards means that the stroke of the push pull rod will act higher up in the slot and thus further away from the hinge. This will naturally result in a smaller flapping angle. A smaller flapping angle means that some shaft torque needs to be transferred directly to the blades in order to keep the rotor at its required rpm. This will cause a yaw movement.

The same holds for a shift of the upper plate downwards: the fixed stroke of the push pull rod will act closer to the hinge which will result in a larger flapping angle. A larger flapping angle means that the rotor will tend to speed up, and will be slowed down by the fixed rpm of the engine. This way a yaw movement in the opposite direction is achieved. For a more elaborate explanation of yaw control see (Ref 2).

Values for flapping power, blade root angle and mechanical flapping moment.

In order to set the dimensions for the flapping mechanism and to choose the correct materials it will be necessary to calculate the flapping power that needs to be transferred to the blade. When the flapping power is known, the required flapping angle of the blade and the magnitude of the forced flapping moment can be calculated.

According to equation (15) the flapping power can be calculated by summing the induced power and profile power. The latter two can be calculated when using the following values: thrust (*T*) is equal to 50 N, the rotor radius with flapping mechanism included has increased to 83.7 cm, the blade chord (*c*) is equal to 53 mm, the angular velocity of the Ornicopter is set at 136 rad/s (1300 rpm), the rotor solidity (σ) is equal to 0.08, the profile drag coefficient ($\overline{C}_{D_p}$) and the lift gradient (C_{l_α}) are estimated to be 0.01 and 5.43 rad^{-1} respectively, and finally the correction factor for non-constant induced velocity (*k*) is equal to 1.2. The following values then follow for the induced power and profile power:

$$P_i = kT\sqrt{\frac{T}{2\rho\pi R^2}} = 183\,W \tag{40}$$

$$P_p = \frac{\overline{C}_{D_p}\sigma\rho(\Omega R)^3\pi R^2}{8} = 407\,W \tag{41}$$

And consequently the flapping power has to be equal to:

$$P_{flap} = P_i + P_p = 590\,W \tag{42}$$

The rigid blade flapping angle can now be calculated by rewriting equation (33) using the expression for the Lock number (equation (21)) and taking into account that the total flapping power is generated by four blades (*N=4*):

$$\hat{\beta} = \sqrt{\frac{1}{N}\frac{16P_{fl}}{\Omega^3\rho C_{l_\alpha}cR^4}} = 4.17^\circ \tag{43}$$

This means that if the demonstrator model would have rigid rotor blades, the forced flapping mechanism should allow for a forced flapping angle equal to 4.17 degrees. However, the blades will not be rigid but will be flexible, and therefore

the calculated rigid flapping angle should, according to equation (35), be multiplied by a factor 5 yielding a forced flapping angle at the blade root equal to approximately 20 degrees.

The windtunnel model on the other hand only yielded a factor 1.5 which in this case would result in a flapping angle equal to 6.3 degrees. This all means that in reality one can expect a forced flapping angle anywhere between 6.3 degrees and 20 degrees. This range proved to be too large for a single design. Therefore the choice was made to focus on the lower part of this flapping angle range, but to make the design modular so that parts can be easily replaced in order to accommodate the higher values of the flapping angle range.

To conclude the calculations the required flapping moment will be calculated. The expression for the non-dimensional flapping moment can, using equation (33) and (21), be written as:

$$\hat{m}_{fl} = \frac{\gamma}{8}\hat{\beta} = \frac{\rho C_{l_\alpha} c R^4}{8I}\hat{\beta} \qquad (44)$$

It now follows for the flapping moment (equation (25)):

$$M_{fl} = \frac{\rho C_{l_\alpha} c R^4}{8}\Omega^2\hat{\beta} = 29 Nm \qquad (45)$$

All parts in the forced flapping mechanism thus have to be designed in such a way that they can withstand a forced flapping moment equal to 29 Nm.

Spring stiffness of the flapping mechanism.

To avoid too much unwanted flapping cross coupling the requirement was set that the flexibility of the blades should be such that equation (38) is true. To check this requirement the stiffness of the rotor blade (*EI*) was measured and found to be equal to 11.81 Nm^2. Since the offset of the blade (*e*) is 18.8% of the total rotor radius the Southwell coefficient can also be calculated:

$$\alpha = 1 + \frac{3}{2}\frac{e}{1-e} = 1 + \frac{3}{2}\frac{0.188}{1-0.188} = 1.346 \qquad (46)$$

The natural frequency of a flapping and rotating rotor blade then is equal to (equation 39):

$$\omega_n = \sqrt{12.37\frac{EI}{mR^4} + 1.346\ \ \Omega^2} = 161.85 \qquad (47)$$

rad/s

with *m* the mass per unit length of the blade equal to 0.25 kg/m. According to the requirement the natural frequency should be smaller than:

$$\omega_n \leq 1.1\ \ \Omega = 1.1*136.1 = 149.71 \text{ rad/s} \qquad (48)$$

This implies that the requirement is not met. Therefore special care should be given to cross-coupling effects during testing.

Final design.

All calculations and drawings have finally resulted in the forced flapping mechanism as shown in figure 15.

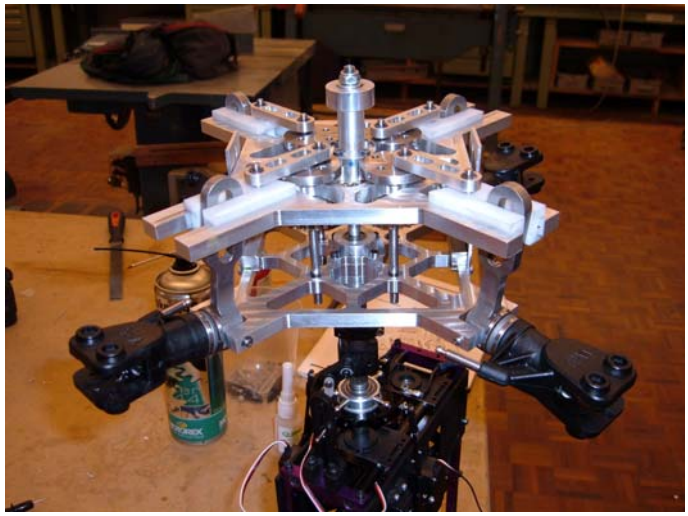

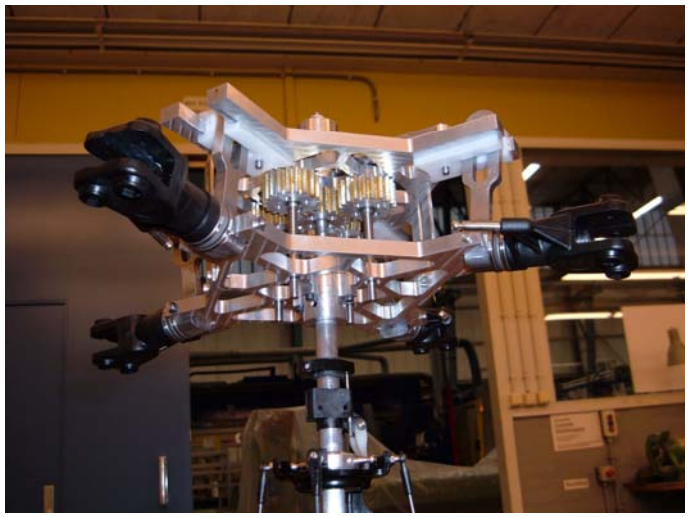

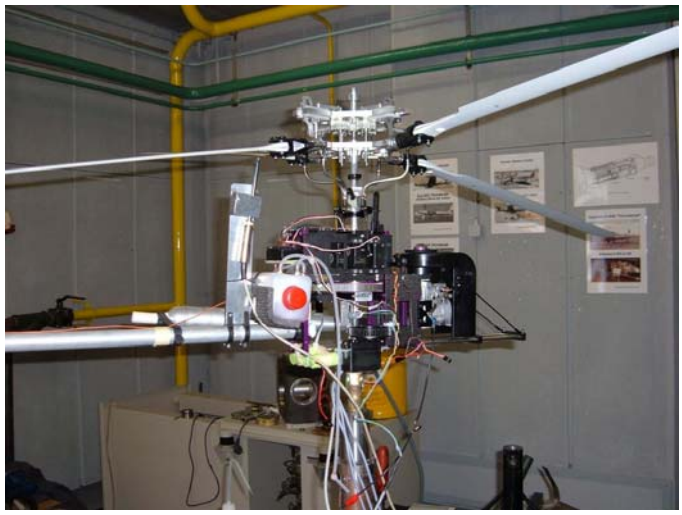

Figure 15: Pictures of the free-flying radio-controlled scale model of the Ornicopter

Tests performed with the radio-controlled Ornicopter

The first tests with the free-flying radio-controlled scale model of the Ornicopter have been performed and yielded very promising results. These results will be discussed in this section.

General test set-up

Although the radio-controlled Ornicopter is designed as a free-flying model, the first tests have been performed with the model firmly attached to a test bench. Since there was no windtunnel present all test results that will be discussed are valid for the hover situation. The variables that have been measured during the tests are: reaction torque on the fuselage, reaction torque on the fixed gearwheel, vertical force, rpm of the rotor, pitch angle of the blades and flapping angle at the root of the blades.

During the tests the rotor blades were rotating at approximately 500 rpm. This is slower than the intended 1300 rpm for which all previous calculations have been performed. The reason to choose this lower rpm is simply to gain insight into the behavior of the rotor blades at a low rpm before proceeding to higher rotational speeds.

The corresponding Reynolds numbers are in the range of 1.6 10^5 with tip Mach numbers of approximately 0.13. The profile drag coefficient C_{D_p} was in the order of 0.035. It should however be mentioned that this profile drag coefficient was derived from the test results using a correction factor for the non-uniformity of the induced velocity (k) equal to 1.2. It is however very well possible that this factor deviates from the usual 1.2 due to the flapping of the blades. Therefore the actual profile drag coefficient can also differ from the calculated 0.035.

Vibrations

As a first striking result it was immediately clear (when looking at the operating Ornicopter model) that all vibrations that were present during the earlier windtunnel tests had disappeared. No vibrations were detected at all, except, of course, the 2P vibration in the torque. It appeared however, that even this vibration was less severe than expected. This was due to the fact that part of the 2P torque vibration was already absorbed by some flexibility in the forced flapping mechanism which allowed the rotor blades to slightly speed up and slow down whereas the calculations assumed an exactly constant rotational speed. Another contribution came from the distribution belts running from the engine to the rotating shaft, these two belts also absorbed a part of the 2P torque vibration.

Reaction torque on fuselage and yaw control

Another important question of course was whether the reactionless situation could be achieved with the new Ornicopter model. Figure 16 shows that this indeed was possible. For a collective pitch angle of 4 degrees a forced flapping angle of approximately 8 degrees was required to obtain the torqueless situation. It can also be seen that the higher the collective pitch, the higher the forced flapping angle needs to be to achieve a situation without reaction torque. Figure 17 shows that the rotor is still producing a lifting force in the torqueless situation.

Figure 16 also illustrates that both a negative and a positive reaction torque on the fuselage can be achieved. When looking at the data point representing 4 degrees collective and 8.3 degrees flapping, it can be seen that an increase in flapping angle to 9.8 degrees while maintaining 4 degrees collective will yield a negative reaction torque whereas a decrease in flapping angle to 7.2 degrees (with 4 degrees collective) will yield a positive reaction torque. Yaw control is thus possible in both directions.

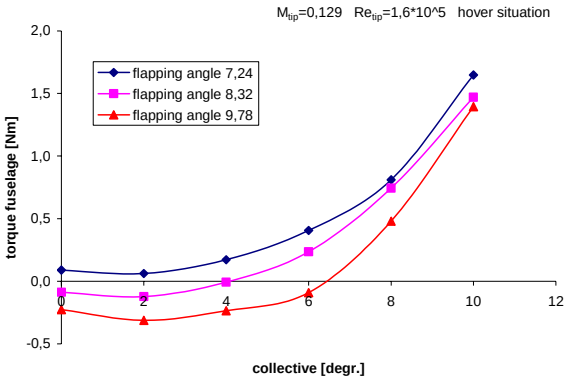

Figure 16: Reaction torque on fuselage as a function of collective

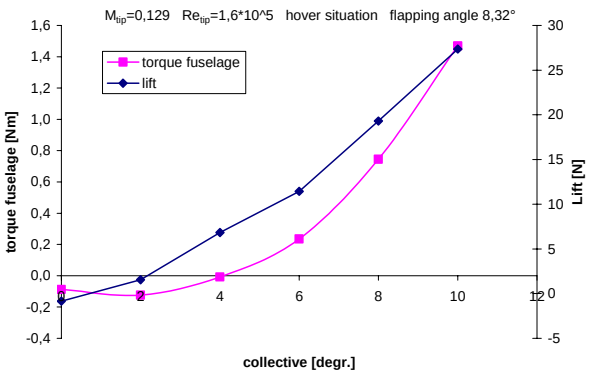

Figure 17: Reaction torque on fuselage and corresponding lift force for a forced flapping angle of 8.3 degrees

Lift

Figure 18 illustrates that the thrust coefficient only depends on the collective pitch and is independent of the forced flapping angle, as could be expected. The same of course holds for the lifting force on the rotor which is depicted in figure 19. It can be seen that the largest lifting force obtained so far (at 500 rpm) is equal to approximately 27 N. The largest lift force that was achieved in the torqueless situation is equal to approximately 13 N (achieved with approximately 6.5 degrees collective pitch and 9.8 degrees flapping). The lift force required for lift off should be equal to 50 N, this will be achievable at the higher rotational speed of the rotor of approximately 1300 rpm.

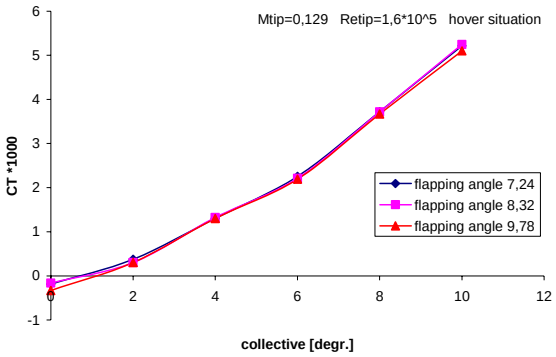

Figure 18: Thrust coefficient as a function of collective and flapping angle.

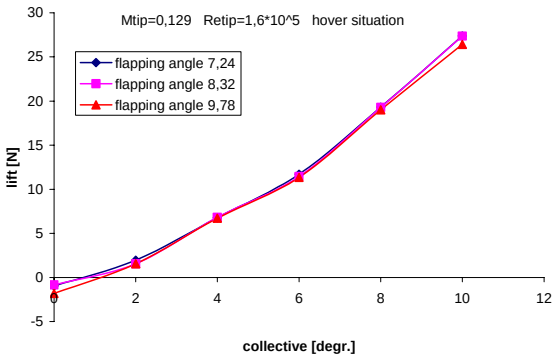

Figure 19: Lift as a function of collective and flapping angle.

Figure of Merit and power required

Looking at figure 20 it can be seen that the magnitude of the forced flapping angle has an influence on the figure of merit, in the sense that the figure of merit decreases with increasing forced flapping angle. This effect can be due to two different causes: either the profile drag coefficient is influenced by the continuous fluctuation of the lift or the correction factor for the non-uniformity of the induced velocity (k) is influenced by this fluctuation or both. At this moment in time it is not yet possible to pinpoint the exact (combination of) cause(s).

Figure 21 additionally gives an indication of the required flapping power. Note that only two points in this graph represent a torqueless situation. The values in figure 21 however, can not be compared to the calculated value in equation (42) due to the difference in rotational speed. Because of the uncertainty in the values for the profile drag coefficient and the correction factor for the non-uniformity of the induced velocity as discussed previously there is no added value in recalculating the flapping power in equation (42) for the correct rotational speed. Therefore a comparison between the tests and theory can not be made at this moment.

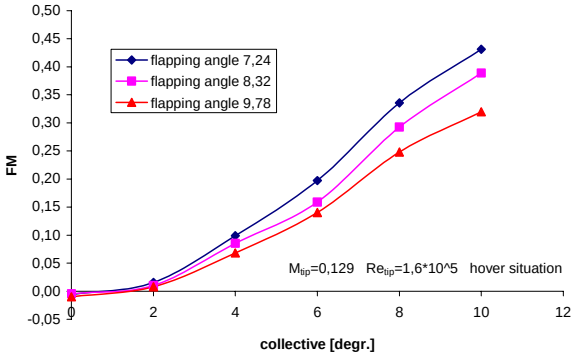

Figure 20: Figure of Merit as a function of collective and forced flapping angle

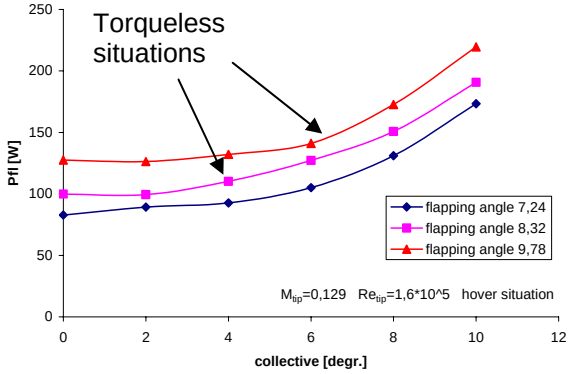

Figure 21: Flapping power as a function of collective and flapping angle.

Required flapping angle

As seen previously, the torqueless situations were achieved with forced flapping angles equal to 8.3 degrees and 9.8 degrees. Again these values can not be compared to equation (43) because of the difference in rotational velocity of the rotor blades. However, in this case the theoretical values for the forced flapping angles can be recalculated using the results of the tests. The rigid blade flapping angles can be calculated with equation (43) when the flapping power that was needed during the tests is substituted, this flapping power is given in table 1.

Table 1: Flapping angle according to rigid blade theory and flapping angle according to tests for the two torqueless situations.

	Collective pitch [deg]	Flapping power test [W]	Flapping angle theory [deg]	Flapping angle test [deg]
Sit. 1	4	110	7.5	8.3
Sit. 2	6.3	150	8.7	9.8

Now it can be seen that there is only about 10% difference between the rigid blade flapping angles as predicted by the theory and the flapping angles that actually occurred during the tests. This is less than was predicted by the flexible blade theory.

Spring stiffness of the flapping mechanism

Earlier in this paper it was noted that special care should be given to cross-coupling effects during testing. So far, the cyclic control of the Ornicopter model has not yet been tested and therefore no conclusions can be drawn regarding these cross coupling effects.

Conlusions and recommendations

The radio-controlled Ornicopter model has been successfully designed, built and tested. The tests showed that all vibrations that occurred during testing of the earlier windtunnel model had disappeared due to the new flapping configuration of the rotor blades. Additionally, the radio-controlled Ornicopter model has a flapping mechanism that is much lighter and much more compact than the flapping mechanism that was used for the windtunnel model. Therefore it is the expectation that this radio-controlled model will actually become a free-flying model in the near future.

The tests demonstrated that a torqueless situation can be achieved while using only modest forced flapping angles, and that yaw control is still possible.

However, the tests also revealed a couple of points of attention that require further research. Firstly, it should be investigated whether an increase in forced flapping angles decreases the figure of merit due to an increase in profile drag coefficient or due to an increase in the correction factor for the non-uniformity of the induced velocity. Secondly, it should be studied why there is only a difference of 10 percent between the flapping angles that were calculated from theory for rigid blades and the flapping angles that occurred during the tests.

Additionally, further tests should be performed in order to determine whether the cross coupling effects that are predicted by the theory actually occur in reality. Tests should also be performed with the model operating in normal helicopter mode in order to be able to compare the results of the Ornicopter mode (with forced flapping of the blades) with the helicopter mode. This way it will be possible to determine whether the Ornicopter mode requires a different amount of power or produces a different amount of lift than a normal helicopter.

References

[1] Holten, Th. van, *A Single Rotor without Reaction Torque: a Violation of Newton's Laws or Feasible?,* 28th European Rotorcraft Forum, Bristol, United Kingdom, 2002

[2] Holten, Th. van, Heiligers, M.M., Waal, G.J. van de, *The Ornicopter: A Single Rotor without Reaction Torque, Basic Principles,* 24th International Congress of the Aeronautical Sciences, Yokohama, Japan, 2004

[3] Holten Th van, Heiligers MM. *Configuration analysis of a torqueless helicopter concept*, 24th *ICAS Congress*, Yokohama, Japan, August-September 2004.

[4] Holten Th van, Heiligers MM, *The influence of flexible blades on the characteristics of the Ornicopter.* 30th European Rotorcraft Forum 2004

[5] Theo van Holten, Monique Heligers, Rolf Kuiper, Stuart Vardy, Gerard Jan van de Waal, Jeroen Krijnen, *Forced Flapping Mechanisms for the Ornicopter: A Single Rotor Helicopter without Reaction Torque*, 30th European Rotorcraft Forum, Marseille, France, 2004

[6] Waal GJR. van de. *Development and Testing of the Ornicopter Wind Tunnel Model, Thesis Report*, Delft University of Technology, Faculty of Aerospace Engineering, 2003.

[7] http://www.ornicopter.nl